

# New design electro-catalytic digital baffle batch oxidation reactor for organic removal from refinery wastewater

Mogdam Gassy Hussein<sup>1</sup>, Amer T. Nawaf<sup>2\*</sup>, Ali Saleh Jafer<sup>3</sup> and Ali A. Hassan<sup>3,4</sup>

<sup>1</sup>Applied Chemistry, College of Applied Sciences–Samarra University–Iraq

<sup>2</sup>Petroleum and Gas Refinery Engineering Department, College of Petroleum Process Engineering, University of Tikrit, IRAQ

<sup>3</sup>Chemical Department, College of Engineering, University of Muthanna, Muthanna, IRAQ

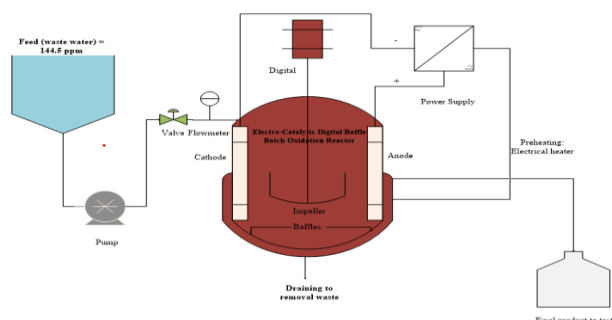
<sup>4</sup>College of Engineering, Al-Ayen University, Thi-Qar, IRAQ

Received: 30/12/2024, Accepted: 19/03/2025, Available online: 26/03/2025

\*to whom all correspondence should be addressed: e-mail: Amer.Talal@tu.edu.iq

<https://doi.org/10.30955/gnj.07218>

## Graphical abstract



## Abstract

A novel design Digital Baffle Electro Catalytic Batch Oxidation Reactor (DBECB) has been conceived to upsurge the specifications of refinery wastewater (RWW), through the removal of organic pollutants by electro catalytic oxidation treatment. The modern design that eliminates organic from RWW with improving its qualities has drawn a lot of attention. These days, one of the things that the world needs are the production of clean water with strict limitations on dangerous compounds. The degree of chemical oxidation that has been used to purify this wastewater is reflected in the electro- catalytic oxidation (ECO) process. The experimentations were intended by a Response surface method experimental design comprising the consequence of the time (10-40) min, magnetite Nano particles (0.1–0.5) gm, temperature (25-60)°C, and pH (3-9) under 0.5 Amps and 200 rpm then examining the results by Minitab software of response surface method with Box Behnken design (BBD) to find the best values of these conditions (40 min, 0.5 gm of nano particle, 3 pH, and 60°C of temperature). The organic elimination efficiency of electro catalytic oxidation was 98.2%. The electro catalytic process was suitable for organic compounds removal from refinery wastewater.

**Keywords:** Crude oil, wastewater treatment, iron, electro-oxidation, DBBR, optimization, BBD

## 1. Introduction

The environmental impact of oilfield plant industries is still often undesired; in the short term, they require a lot of water and generate a lot of oily waste water, which is a serious issue for oil manufacturing facilities and the environment (Hassan and I. K. Shakir 2024). The types of organic forms that are present, the physical method the water was bent, and the location all affect the refinery wastewater's characteristics (Hassan *et al.* 2019). Overall, more stringent environmental regulations require oil and gas companies to take a variety of RWW actions prior to reservoir inoculation and earlier notice in order to reduce created injury (Hassan and Naeem 2018). Water that has been properly maintained can now be recycled and used for water flooding. There are many problems with the conservative separation methods because of some contaminants are dangerous, non-biodegradable, and rowdy, these methods are less real at removing them from refinery wastewater (Farise *et al.* 2021). However, none of these methods of treatment was adequate to contaminate water with adequate concentrations of the most persistent contaminants. Frequently, further therapy steps are required to achieve this goal coagulation (Al-Hassan and Shakir 2024), flotation (AlJaberi *et al.* 2023), and membrane treatment are just a few of the industrialized methods used to remove heavy metal from wastewater (Alardhi *et al.* 2024). However, because the membrane is still contented to place and works finished scums with poor competence, the use of membrane separation procedures has limitations (Hassan *et al.* 2020). The disadvantage of the precipitation process is its high cost, which consequences from the addition of numerous components (Farooq *et al.* 2010). As a result, more authors focus on honing their methods for removing organic complexes from refinery wastewater by hybrid methods of adsorption and oxidation (Mary *et al.* 2022). Magnetic nanoparticles (MNPs) are an interesting class of nanomaterials that have been widely researched for usage in numerous industrial applications (Naser *et al.* 2021). MNPs have been applied in sensing technologies,

memory storage devices, magnetic separation, magnetic labeling, and catalytic processes. MNPs have been employed in biological applications to give contrast effects for magnetic imaging, to remotely control targeted drug administration, and to produce warmth for the treatment of hyperthermia (Jun *et al.* 2020). Iron oxide nanoparticles (NPs) are a potential class of magnetic materials because of their high biocompatibility. The primary motivation for significant research efforts to commercialize iron oxide nanoparticles for enhanced medical technology applications is their biocompatibility. While there are many other kinds of iron oxides, the term "iron oxides" usually refers to three types:  $\text{Fe}_3\text{O}_4$  (Xu and Lee 2021).

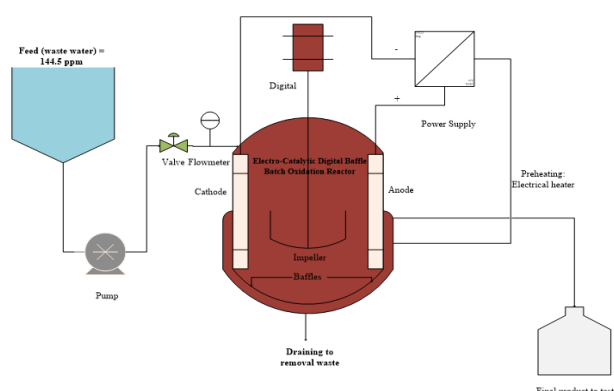
Advanced oxidation processes (AOPs) have been unable to overcome the disadvantages of conservative methods in previous decades (Alturki *et al.* 2024). Under sensible conditions, these methods can eliminate the pollutants into innocuous inorganic elements that are unconfined as  $\text{CO}_2$  and  $\text{H}_2\text{O}$  and sludge (Ibrahim *et al.* 2023). In rural areas, AOPs are essentially physicochemical processes that generate a lot of oxidizing species, chiefly free radicals ( $\bullet\text{OH}$ ), which have the highest potential for oxidation (Alamery and Hassan 2022). The conduct of advanced oxidation processes, which are based on extremely reactive radicals, has remained relatively well defined at near ambient temperature (Hassan and Al-Zobai 2019). Intractable pollutants in the wastewater

**Table 1.** Properties of refinery wastewater

Working	value	Working	value
Organic concentration	155.4 ppm	density	0.997
Turbidity	44.2 NTU	conductivity	72357 $\mu\text{S}/\text{cm}$
pH	6.85	TSS	17.2 (ppm)
Dissolved oxygen content	0.045 (ppm)	viscosity	1.05 m Pa. $\text{S}^{-1}$

**Table 2.** The specifications of the DBBBR

Description	Specification
Reactor dimension	Height = 13 cm, Diameter = 9 m
Rod length	30 cm
Kind of impeller (Stainless steel)	Four basket impeller
Basket height	1.15 cm
Basket length	1.2 cm
Basket width	1.2 cm
Diameter of Impeller	85 mm
Baffle height (Stainless steel)	8 cm
Baffle width	1.3–1.4 cm



environment can be wickedly soiled by AOPs (Sultan *et al.* 2020). This work was interested in organic elimination from refinery wastewater by new design of Digital Baffle oxidation of the electro-catalytic/oxidation treatment with working variables of the time, Nano particles, pH, and temperature using response surface method.

## 2. Experimental work

### 2.1. Chemical and logical examination

$\text{Fe}_3\text{O}_4$  nano particles supplied from ACS material, HCL (Scharlau, Spain 98 % purity) and NaOH (Scharlau, Spain, 97% purity). The refinery wastewater came from the oil station's clearing at Al-Muthanna Oilfield in Iraq, which is home to the wet oil unit. It was kept in a polypropylene ampule on its own and maintained at  $4^\circ\text{C}$  to keep the properties of RWW and shown in **Table 1**. To break up the organic emulsion, 40 milliliters of wastewater and 0.2 grams of NaCl were injected at the conclusion of each experiment. Four milliliters of  $\text{CCl}_4$  were added, and it was shook violently for two minutes. After the solution was separated into two distinct coats after 20 minutes, the bottom (organic) layer was employed for the absorbance test, and the calibration curve was used to identify the organic (Alakoul *et al.* 2021).

**Figure 1.** Hybrid adsorption and oxidation reactor

### 2.2. Novel design of pilot plant (DBEBR)

The Digital Baffle Electro Batch Reactor (DBEBR) was designed in the Faculty of Engineering, Chemical Engineering Department, University of Al Muthanna, and Muthanna, Iraq to produce water clean by removing organic compounds from the wastewater via electro-catalytic oxidation. In this work, we have designed the new reactor of different workings of the reactor. Assessment of the efficiency of the reactor in the context of RWW treatment via electro coagulation/ oxidation method is one of the aims of this study. The DBEBR design achieved a high mass transfer rate in the electro-oxidation

process and improved the distribution of iron in wastewater. In the DBEBR design, a rod was attached to the digital mixer (which had an impeller speed range of up to 3000 RPM), and the end of the rod was connected to the three-baffle impeller. Following that, the baffle represented a good equal distribution at the end of the rod with the (8 cm, 4cm, and 0.11cm) of aluminum and (8 cm, 3 cm, 0.12 cm) of iron as anode and cathode respectively. By increasing the amount of transfer reactants inside the reactor, these baffles improve the effectiveness of the electro-adsorption/oxidation technique. Additionally, three baffles were added to the reactor wall to prevent stagnant zones from developing and to encourage a chain reaction among the reactants. Equally, spaced baffles were placed inside the reactor's surface, with 36 cm between each pair. The reactor was also insulated using a 2.5 cm protrusion of woolen material (for high temperatures above 1000°C). Stainless steel was used to build the reactor. **Table 2** contains a list of the DBBBR's specifications, and **Figure 1** shows the system's schematic.

### 2.3. Hybrid treatment

A UV spectrophotometer (UV-1800 Shimadzu, Japan) was used to monitor the variation in the organic concentration in RWW during the adsorption and oxidation system procedure. The results were reconstructed into the conforming concentrations (C). Equation (1) was used to compute the organic efficiency.

$$\eta = \frac{C_o - C_t}{C_o} \times 100 \quad (1)$$

Where  $\eta$ , percentage of organic removal;  $C_o$  and  $C_t$ , measured concentration before the and after treatment (ppm) respectively.

Response surface methodology, which is equivalent to statistical software (Minitab-17), was used to design the trials and forecast the outcomes of the working factors separately and in relation to one another. The primary factors influencing these problems, namely the electrolysis-oxidation time ( $X_1$ ), pH ( $X_2$ ), iron concentration ( $X_3$ ), and hydrogen peroxide ( $X_4$ ), were purposefully rendered according to the ranges shown in **Table 3**.

**Table 3.** Working parameters

Working	Ranges
$X_1$ : time (min)	10-40
$X_2$ : pH	3-9
$X_3$ : Iron dose (gm)	0.1-0.5
$X_4$ : Temperature	25-60

## 3. Results and discussion

### 3.1. Characterization of nano-Fe<sub>2</sub>O<sub>3</sub>

#### 3.1.1. FESEM Result for Fe<sub>2</sub>O<sub>3</sub>-nanoparticles

FESEM determines the surface shape and active metal dispersion between them. The nano-particles (Fe<sub>2</sub>O<sub>3</sub>) surface mapping produced by FESEM is shown in **Figure 2**, which displays a superb distribution of active components. The precipitation technology is an effective

way to create this kind of catalyst with good active metal dispersion (Hassan and Shakir 2024). The catalyst's surface morphology is depicted in Figure 5.7; the surface's shape is spherical.

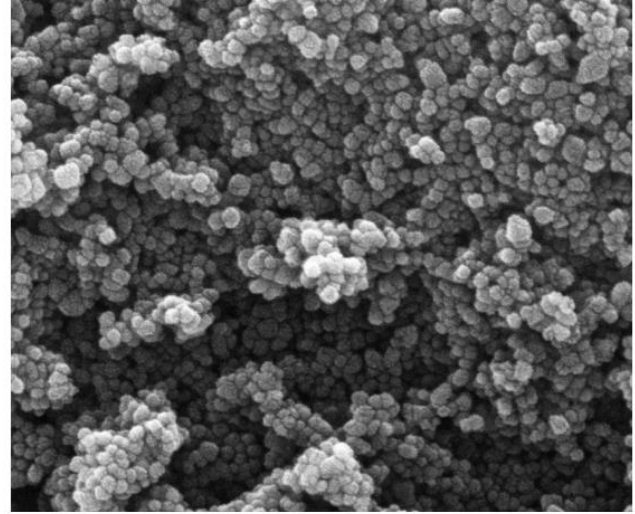


**Figure 2.** FESEM result for Fe<sub>2</sub>O<sub>3</sub>-particles

#### 3.1.2. FTIR results for Fe<sub>2</sub>O<sub>3</sub>-nanoparticles

**Figure 3** displays the results of FTIR analysis for the synthetic nano-Fe<sub>2</sub>O<sub>3</sub> in the 4000-500 cm<sup>-1</sup> wave number range. It was determined that the O–H stretching vibration was responsible for the band at 3500-3000 cm<sup>-1</sup>, whereas the H–O–H symmetric stretching vibration of adsorbed water molecules was responsible for the band at about 1645 cm<sup>-1</sup>. As seen in **Figure 3**, the stretching vibrations of Fe–O–Fe, which are typical of Fe<sub>2</sub>O<sub>3</sub>, are responsible for the absorption bands centered at 440, 580, and 620 cm<sup>-1</sup> (Rashid *et al.* 2020).

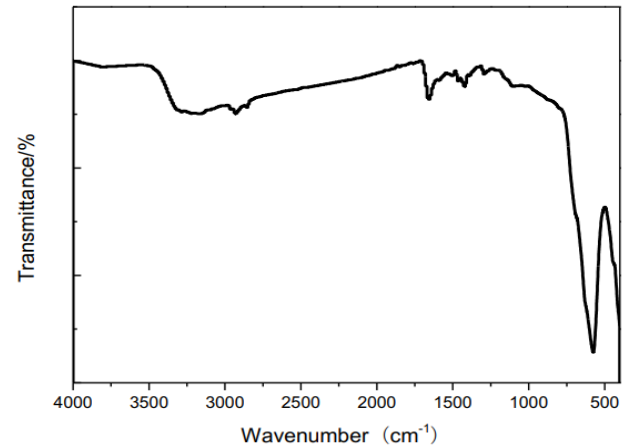


**Figure 3.** FTIR result for Fe<sub>2</sub>O<sub>3</sub> nano-particles

#### 3.1.3. XRD result for Fe<sub>2</sub>O<sub>3</sub> nano-particles

The XRD pattern of the synthesized nano Fe<sub>2</sub>O<sub>3</sub> nano-particles (commercial supplied) is displayed in **Figure 4**. Clearly visible as large peaks at  $2\theta$  angles approximately (31.234°, 38.02334°, 43.432°, 58.9283° and 62.3465°), respectively, are the many primary reflections of the nano Fe<sub>2</sub>O<sub>3</sub> phase. The pattern's peaks clearly show that Fe<sub>2</sub>O<sub>3</sub> crystallites of nanoscale size have formed. This behavior demonstrated a strong dispersion of molecules supported

by Fe<sub>2</sub>O<sub>3</sub> on the catalyst surface (Nawaf and Abdulmajeed 2024).

The working variable settings, the final organic concentration in wastewater (27 tests were conducted by BBD), and the elimination efficiency targeted at adsorption and oxidation treatment run are explained in **Table 4**. The mathematical equation (Eq. 2) was manufactured in terms of actual factors associating the copper removal response to the active variables, representative the interconnections between these variables, and was founded on investigative consequences:

$$\begin{aligned} \text{Organic Removal} = & 16.2 + 2.45X_1 + 0.773X_2 + 1.33X_3 + 3.73X_4 \quad (2) \\ & - 0.0469X_1^2 - 0.00447X_2^2 - 0.0075X_3^2 \\ & - 0.766X_4^2 - 0.0022X_1X_2 - 0.0089X_1X_3 \\ & + 0.038X_1X_4 + 0.004X_2X_3 - 0.0182X_2X_4 \\ & - 0.055X_3X_4 \end{aligned}$$

ANOVA is demonstrated in **Table 5** with a focus on the electro catalytic oxidation response surface model. The results of the Fisher-value, P-test, adjusted sum of squares, adjusted mean of squares, degree of freedom, and sum of squares for all parameters are shown in **Table 5**. Just 4.33 percent of the total variants are not reinforced by schooling, according to the model's multiple correlation constant, which is 92.5% compatible with the statistical significance of the regression. **Figure 5** shows that the adjusted manifold correlation coefficient (adj. R<sup>2</sup>

**Table 4.** Results of the BBD experiments

NO	Time (min) X <sub>1</sub>	Dose (gm) X <sub>2</sub>	Temperature X <sub>3</sub>	pH X <sub>4</sub>	Organic removal by ECO (%)
1	10	0.1	43	6	64.2
2	40	0.1	43	6	77.3
3	10	0.5	43	6	78.5
4	40	0.5	43	6	88.2
5	25	0.3	25	3	84.1
6	25	0.3	60	3	96.3
7	25	0.3	25	9	73.8
8	25	0.3	60	9	80.3
9	10	0.3	43	3	90.4
10	40	0.3	43	3	98.2
11	10	0.3	43	9	77.8
12	40	0.3	43	9	89.1
13	25	0.1	25	6	83.8
14	25	0.5	25	6	93.5
15	25	0.1	60	6	94.6
16	25	0.5	60	6	98.5
17	10	0.3	25	6	86.4
18	40	0.3	25	6	93.4
19	10	0.3	60	6	96.8
20	40	0.3	60	6	98.9
21	25	0.1	43	3	88.7
22	25	0.5	43	3	99.3
23	25	0.1	43	9	84.5
24	25	0.5	43	9	94.6
25	25	0.3	43	6	95.1
26	25	0.3	43	6	94.2
27	25	0.3	43	6	93.9

= 91.3%) and R<sup>2</sup> matched well in this model (Altunay *et al.* 2021).

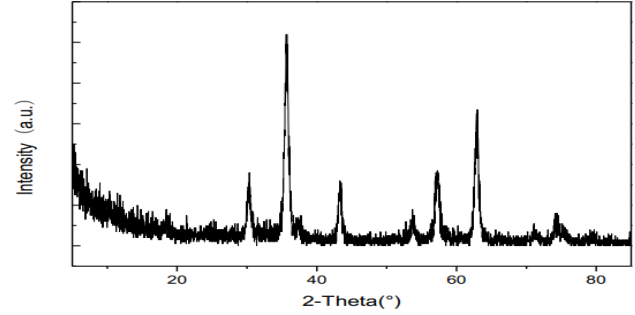


**Figure 4.** XRD result for Fe<sub>2</sub>O<sub>3</sub> nano-particles

The results in **Figure 6** explain that the high competence response of elimination along the time of oxidation aimed at all values of the organic removal, the hybrid effects of dose and temperature, and time at acid solution had a strong interaction directed towards metal elimination and vice versa to pH on the organic removal when increasing the pH led to decrease the organic removal. This is because there are insufficient locations on the adsorption and oxidation of steel steel and iron as anode and cathode correspondingly, and the free radical from electro-oxidation is more compared to adsorption and oxidation method substantial surface to achieve a relatively high elimination ratio (El Kaim Billah *et al.* 2023)

The data were analyzed using the "Minitab 17" application, and the main conclusions regarding the issues were consistent. The change in response resulting from a change in the level of an issue still determines its outcome. This is commonly referred to as the major effect because it tackles the primary issues of interest in the experiment (Jafer *et al.* 2023). **Figure 7** demonstrate the key components of each restriction on the organic removal. The iron dose, temperature, pH, and duration had the biggest effects on the elimination of organic in RWW. In the range under study, this constant, which has a positive sign, indicates how rising concentrations of iron dose and temperature as well as time would increase organic removal and, on the other hand, how increasing pH would decrease organic removal (Kurniawan *et al.* 2023).

**Table 5.** ANOVA for organic removal

Foundation	DOF	Seq. SS	Adj. MS	Fisher Value	P-test Value
1-Model	14	1253.56	89.54	1.34	0.309
Linear	4	994.9	248.725	3.72	0.034
$X_1$	1	218.79	218.787	3.27	0.096
$X_2$	1	297.89	297.889	4.45	0.056
$X_3$	1	211.68	211.68	3.17	0.101
$X_4$	1	266.55	266.545	3.99	0.069
Square	4	237.37	59.342	0.89	0.501
$X_1^2$	1	147.93	147.935	2.21	0.163
$X_2^2$	1	105.81	105.811	1.58	0.232
$X_3^2$	1	0	0	0	0.999
$X_4^2$	1	48.94	48.938	0.73	0.409
2-Way Interaction	6	26.9	4.484	0.07	0.998
$X_1 * X_2$	1	2.89	2.89	0.04	0.839
$X_1 * X_3$	1	5.46	5.459	0.08	0.78
$X_1 * X_4$	1	3.06	3.063	0.05	0.834
$X_2 * X_3$	1	7.9	7.897	0.12	0.737
$X_2 * X_4$	1	0.06	0.062	0	0.976
$X_3 * X_4$	1	7.53	7.532	0.11	0.743
Error	12	802.53	66.877		
Lack-of-Fit	10	801.75	80.175	205.58	0.005
Pure Error	2	0.78	0.39		
Total	26	2056.08			

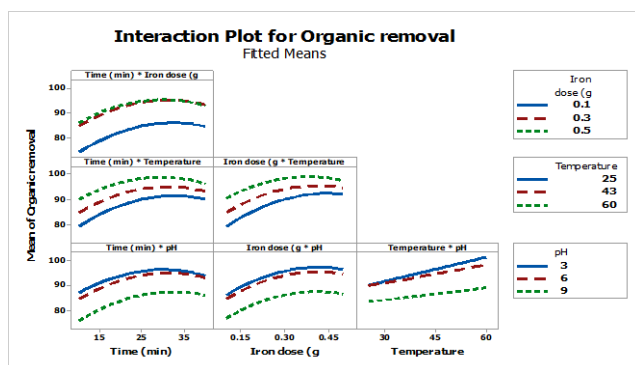


**Figure 6.** Interaction plot of variables of adsorption and oxidation

The ideal settings for best working variables including pH, temperature, iron dose, and time were still established. **Figure 8** displays the measurement effects of the D-

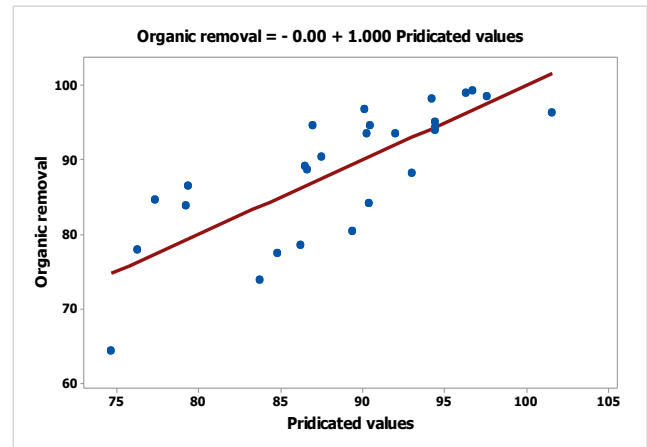


**Figure 5.** Observed vs predicted values of organic removal

optimization for the electro catalytic oxidation of organic pollutants in refinery wastewater (Pinoargote-Chang *et al.* 2022).

### 3.2. Effect of working variables on organic removal

#### 3.2.1. Nano iron dose effect on the removal efficiency

The relationship between the dose and the organic elimination was shown in **Figure 9**. It revealed that the elimination competence increased as the dose increased from 0.1 to 0.5 gm, the all-out elimination competence was 92.3 % at 0.44 gm of  $Fe_3O_4$ , 40 minutes of irradiation time, pH 7, and 60°C. Elimination competence increases with iron because continual amount additions produce high amount that remove organic pollutants in refinery wastewater (Hassan *et al.* 2022).

#### 3.2.2. The effect of pH on the removal efficiency



pH values were substantial impact on the adsorption and oxidation technique. Therefore, a chosen pH variety is required for the procedure to be obtainable in the greatest possible way. The effect of pH on the ability to eliminate organic was explained in **Figure 10**. The findings show that elimination competence increases as pH decreases, with 3.0 being the ideal pH. These theories align with author's findings (Alturki *et al.* 2021) which states that the pH value's impact on organic pollutants removal is still not particularly noteworthy., several experiments were still conducted with variations on the pH range from 3 to 9. The organic elimination efficiency was 93.2% has been preserved at pH=3 and gradually decreased to a pH=9 value just above this threshold. The combined methods had demonstrated a clear decrease in organic elimination of 82.5%. Given that the maximum amount of organic elimination was determined to be with a pH at an acidic solution (Ahmed *et al.* 2021).

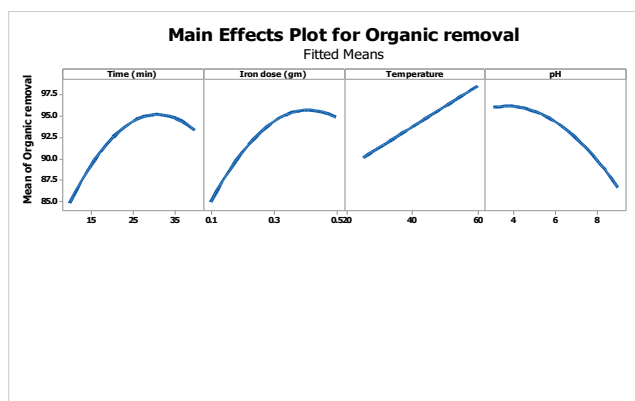


**Figure 7.** Impact main effect of adsorption and oxidation

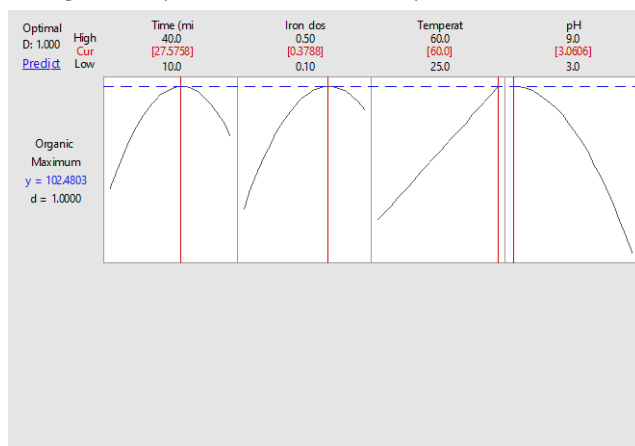


**Figure 8.** The optimum values of the operational variables

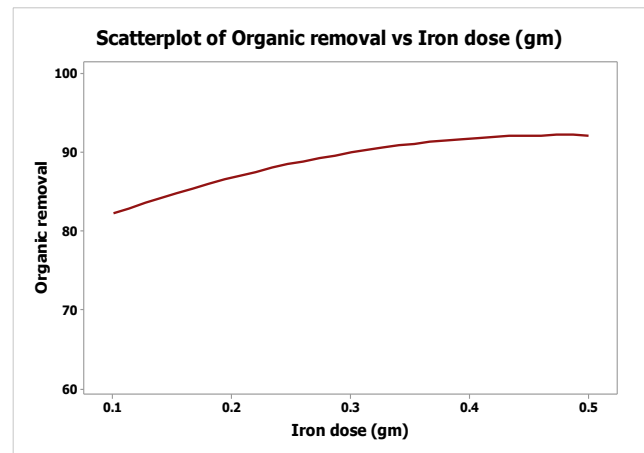


**Figure 9.** Effect of iron dose on the elimination process

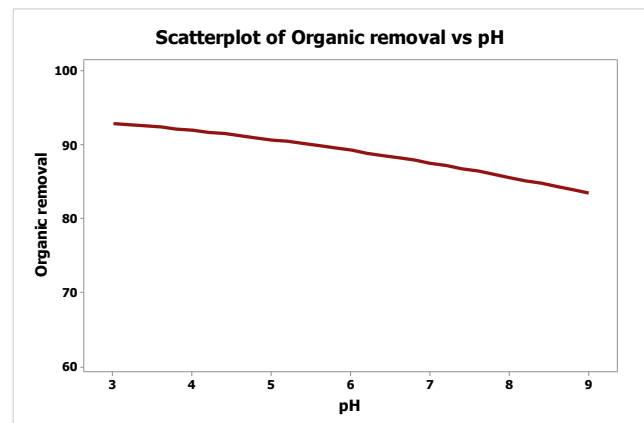


**Figure 10.** Effect of solution pH on elimination of organic compounds

### 3.2.3. The effect of oxidation time on the removal efficiency

It was purposeful to examine the adsorption and oxidation time variable in relation to the oxidation treatment and its impact on the ability to eliminate organic with the breakdown of ion constituents, the free radicals from anode that were created in the oxidation knowledge might quickly oxidize into hardness due to their strong oxidizing capacity (Jasim and Aljaberi 2023). The relationship between oxidation time and organic removal efficiency throughout the action phase is illustrated in **Figure 11**. The outcome was consistent with authors that demonstrated that an increase in oxidation time increases process efficiency, as demonstrated by the findings of Ali *et al.* 2020 (Aljaberi *et al.* 2020).

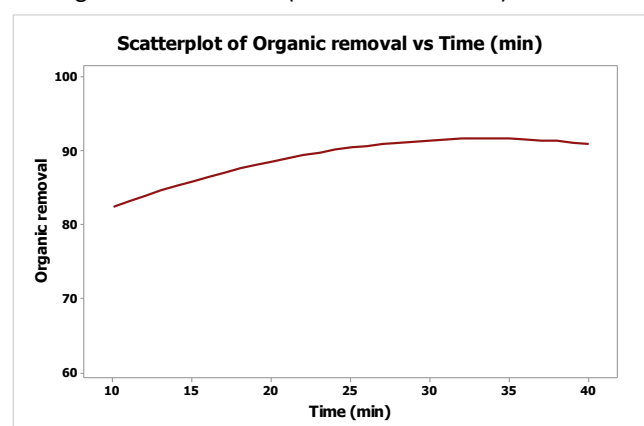


**Figure 11.** Effect of time in the elimination of organic compounds

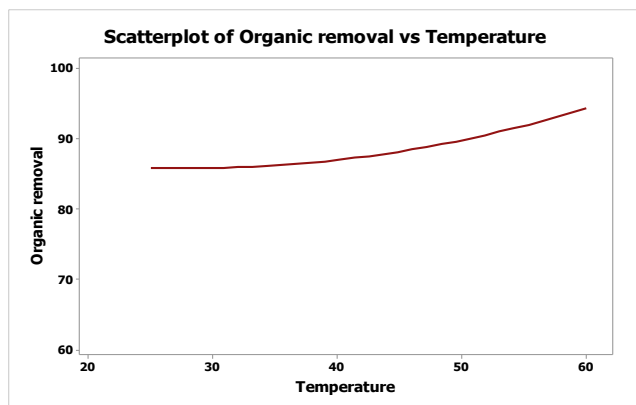


**Figure 12.** Effect of temperature of the organic removal

### 3.2.4. Effect of temperature on the removal efficiency

The wastewater treatment was still impacted by the additional variable of temperature. The effect of varying temperature on the ability to remove organic compounds from refinery wastewater. The elimination competence increased from 84.2% to 93.5 % as soon as the temperature increased from 25 to 60°C. **Figure 12** illustrates that the all-out organic elimination increased with increased temperature (Naeem *et al.* 2018).

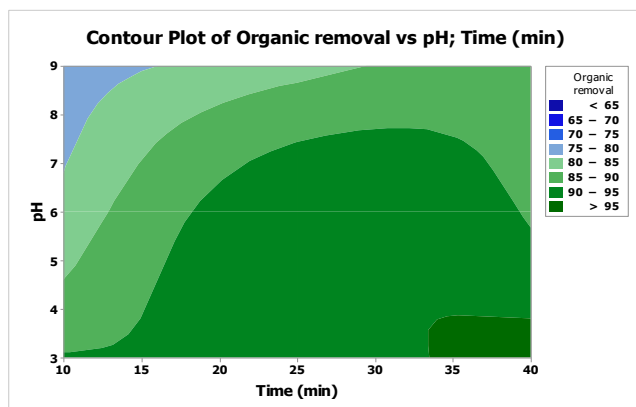


**Figure 13.** Contour plot of organic pollutants vs pH and time

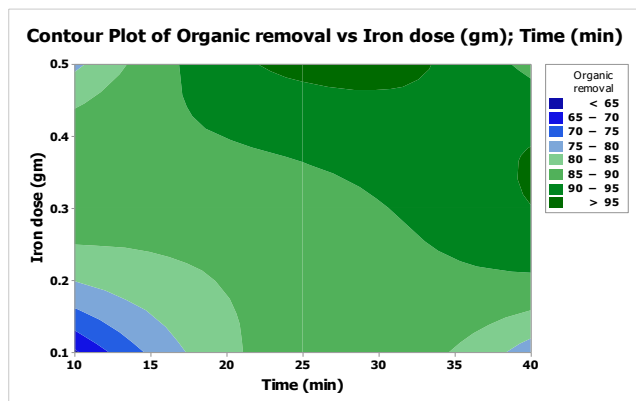


**Figure 14.** Contour plot of organic pollutants vs iron dose and time

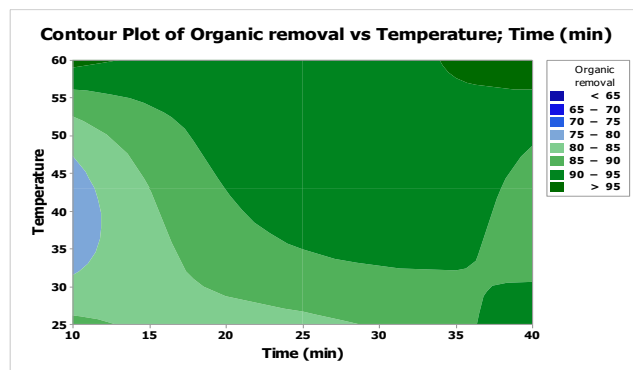


**Figure 15.** Contour plot of organic pollutants vs temperature and time

As shown in **Figures 13, 14, and 15**, respectively, the contour plot for organic removal shows how the x-axis responds to oxidation time and changes with pH, iron dose and temperature. The results of the Figure show that increasing the adsorption and oxidation at acid solution increases organic elimination when compared to the basic solution because free radicals are produced at lower pH, organic compounds in the refinery wastewater are oxidized, and the hybrid treatment efficiency is increased (Al-Khafaji *et al.* 2019). The results indicate that the oxidation reaction is comparatively faster than the adsorption and exhibits rapid elimination of organic molecules (Dawood Salman *et al.* 2023).

## 4. Conclusions

To advance the technology of electro-Fenton oxidation, a novel design of pilot plant Digital Baffle Electro Photo Fenton Batch Oxidation Reactor has been developed. Based on the findings, a new design that improves the mass transfer of copper reactants by Fenton, photo Fenton, and electro Fenton is presented, and their differences are contrasted. All of the intentional answers that show the satisfactory modification of the second order polynomial model must have high regression constants in the mathematical relationships that were discovered. An organized technique for cleaning up solutions with low copper concentrations is still the electro Fenton procedure. It was discovered that the novel DBEPBR design improved oxidant towards organic contaminants in wastewater, leading to 99.3% copper metal removal under mild operating circumstances (pH 3, ferrous Sulphate 18 ppm, electrolysis period 30 min, and hydrogen peroxide 75.8 ppm). This technique can be suggested as an unofficial means of producing water treatment due to the effectiveness of electro-Fenton operation.

## Acknowledgment

This education was financially reinforced finished the Muthanna University, Iraq. The authors approvingly confess the unresolved delivery as long as through the authorities of the workshop in the College of Engineering.

## References

Ahmed I.H., Hassan A.A. and Sultan H.K. (2021). Study of Electro-Fenton Oxidation for the Removal of oil content in refinery wastewater, *IOP Conference Series: Materials Science and*

- Engineering*, **1090**(1), 012005, 2021, doi: 10.1088/1757-899x/1090/1/012005.
- Alakoul K.A., Atiyah A.S., Azeez M.Z. and Hassan A.A. (2021). Photovoltaic cell Electro-Oxidation for Oil Removal in oil field produced H<sub>2</sub>O, *IOP Conference Series: Materials Science and Engineering*., **1090**(1), 012072, doi: 10.1088/1757-899x/1090/1/012072.
- Alamery H.R.D. and Hassan A.A. (2022). Effect of intensity of light and distance for decolonization in direct red wastewater by photo fenton oxidation, *ARP Journal of Engineering and Applied Sciences*, **17**, 1819–6608.
- Alardhi S.M. *et al.* (2024). Artificial neural network and response surface methodology for modeling reverse osmosis process in wastewater treatment, *Journal of Industrial and Engineering Chemistry*., **133**, 599–613, doi: 10.1016/j.jiec.2024.02.039.
- Al-Hassan A.A. and Shakir I. (2025). Enhanced Photocatalytic Activity of CuO/NCW via Adsorption Optimization for refinery wastewater, *Iran. Journal of Chemistry and Chemical Engineering*., **44**(1). Articles in Press.
- Aljaberi F.Y., Abdulmajeed B.A., Hassan A.A. and Ghadban M.L. (2020). Assessment of an Electrocoagulation Reactor for the Removal of Oil Content and Turbidity from Real Oily Wastewater Using Response Surface Method, *Recent Innovations in Chemical Engineering. (Formerly Recent Patents on Chemical Engineering)*, **13**(1), 55–71, doi: 10.2174/2405520412666190830091842.
- Aljaberi F.Y., Hadi D.R. and Ajjam S.K. (2023). Electrocoagulation Treatment of Textile Wastewater: A Review, *AIP Conference Proceedings*., **2806**(1), doi: 10.1063/5.0163278.
- Al-Khafaji R.Q. and Mohammed A.H.A.K. (2019). Optimization of Continuous Electro-Fenton and Photo electro-Fenton Processes to Treat Iraqi Oilfield Produced Water Using Surface Response Methodology, *IOP Conference Series: Materials Science and Engineering*., **518**(6), doi: 10.1088/1757-899X/518/6/062007.
- Altunay S., Kiliç H., Öden M.K. and Çakmak B. (2021). Pollutant removal from mining processing wastewater by electrochemical method, *Glob. Nest Journal*., **23**(2), 178–185, 2021, doi: 10.30955/gnj.003683.
- Alturki S.F., Ghareeb A.H., Hadi R.T. and Hassan A.A. (2021). Evaluation of Using Photovoltaic Cell in the Electro-Fenton Oxidation for the Removal of Oil Content in Refinery Wastewater, *IOP Conference Series: Materials Science and Engineering*., **1090**(1), 012012, doi: 10.1088/1757-899x/1090/1/012012.
- Alturki S.F., Suwaed M.S., Ghareeb A., Aljaberi F.Y. and Hassan A.A. (2024). Statistical Analysis and Optimization of Mechanical-Chemical Electro-Fenton for Organic Contaminant Degradation in Refinery Wastewater, *Journal of Engineering Research*
- Dawood Salman A. *et al.* (2023). Defining the optimal conditions using FFNNs and NARX neural networks for modelling the extraction of Sc from aqueous solution by Cryptand-2.2.1 and Cryptand-2.1.1, *Heliyon*, **9**, (11), doi: 10.1016/j.heliyon.2023.e21041.
- El Kaim Billah R. *et al.* (2023). A Novel Chitosan/Nano-Hydroxyapatite Composite for the Adsorptive Removal of Cd(II) from Aqueous Solution, *Polymers (Basel)*., **15**(6), 2023, doi: 10.3390/polym15061524.
- Farise S.B., Alabdly H.A. and Hasan A.A. (2021). Lead Removal from Simulated Wastewater Using Magnetite As Adsorbent with Box-Behnken Design, *IOP Conference Series: Earth and Environmental Science*., **790**(1), doi: 10.1088/1755-1315/790/1/012020.
- Farooq U., Kozinski J.A., Khan M.A. and Athar M. (2010). Biosorption of heavy metal ions using wheat based biosorbents—A review of the recent literature, *Bioresource Technology*., **101**(14), 5043–5053, doi: 10.1016/j.biortech.2010.02.030.
- Hassan A.A. and Al-Zobai K.M.M. (2019). Chemical oxidation for oil separation from oilfield produced water under uv irradiation using titanium dioxide as a nano-photocatalyst by batch and continuous techniques, *International Journal of Chemical Engineering*., **2019**, doi: 10.1155/2019/9810728.
- Hassan A.A. and Naeem H.T. (2018). DEGRADATION OF OILY WASTE WATER IN AQUEOUS PHASE USING SOLAR (ZnO, TiO<sub>2</sub> and Al<sub>2</sub>O<sub>3</sub>) CATALYSTS, *Pakistan journal of biotechnology*, **15**. December, 927–934.
- Hassan A.A. and Shakir I.K. (2024). Kinetic Insights into Solar-Assisted Fabrication and Photocatalytic Performance of CoWO<sub>4</sub>/NCW Heterostructure, *Bulletin of Chemical Reaction Engineering & Catalysis*., **10**
- Hassan A.A. and Shakir I.K. (2024). Synthesis of Nanocellulose Using Ultrasound-Assisted Acid Hydrolysis for Adsorption/Oxidation of Organic Pollutants in Wastewater Under Uv and Solar Light, *Journal of Sustainability Science and Management*., **19**(12), 120–140, doi: 10.46754/jssm.2024.12.008.
- Hassan A.A., Aljaberi F.Y. and AL-Khateeb R.T. (2022). Batch and Continuous Photo-Fenton Oxidation of Reactive-Red Dye from Wastewater, *Journal of Ecological Engineering*, **23**(1), 14–23.
- Hassan A.A., Hadi R.T., Rashid A.H. and Naje A.S. (2020). Chemical modification of castor oil as adsorbent material for oil content removal from oilfield produced water, *Pollution Research*., **39**(4), 892–900.
- Hassan A.A., Naeem H.T. and Hadi R.T. (2019). A Comparative Study of Chemical Material Additives on Polyacrylamide to Treatment of Waste Water in Refineries, *IOP Conf. Ser. Mater. Sci. Eng.*, **518**(6), 62003, doi: 10.1088/1757-899X/518/6/062003.
- Ibrahim H.A., Hassan A.A., Ali A.H. and Kareem H.M. (2023). Organic removal from refinery wastewater by using electro catalytic oxidation, in *AIP Conference Proceedings, AIP Publishing*.
- Jafer A.S., Al-Khateeb R., Alobaid B., Atiyah A. and Hassan A.A. (2023). Copper removal from produced water by photo Fenton oxidation, in *AIP Conference Proceedings, AIP Publishing*.
- Jasim M.A. and Aljaberi F.Y. (2023). Treatment of oily wastewater by electrocoagulation technology: A general review (2018-2022), *Journal of Electrochemical Science and Engineering*., **13**(2), 361–372, doi: 10.5599/jese.1472.
- Jun K.C., Abdul Raman A. A. and Buthiyappan A. (2020). Treatment of oil refinery effluent using bio-adsorbent developed from activated palm kernel shell and zeolite, *RSC Advanced*., **10**(40), 24079–24094, doi: 10.1039/d0ra03307c.
- Kurniawan T.W., Sulistyarti H., Rumhayati B. and Sabarudin A. (2023). Cellulose Nanocrystals (CNCs) and Cellulose



- Nanofibers (CNFs) as Adsorbents of Heavy Metal Ions, *Journal of Chemistry*, **2023**(1), doi: 10.1155/2023/5037027.
- Mary B.C.J. *et al.* (2022). Study of Barium Adsorption from Aqueous Solutions Using Copper Ferrite and Copper Ferrite/rGO Magnetic Adsorbents, *Adsorpt. Science and Technology*, **2022**, 2022, doi: 10.1155/2022/3954536.
- Naeem H.T., Hassan A.A. and Al-Khateeb R.T. (2018). Wastewater-(Direct red dye) treatment-using solar fenton process, *Journal of Pharmaceutical Sciences and Research*, **10**(9), 2309–2313.
- Naser G.F., Dakhil I.H. and Hasan A.A. (2021). Organic pollutants removal from oilfield produced water using nano magnetite as adsorbent, *Global NEST Journal*, **23**(3), 381–387, doi: 10.30955/gnj.003875.
- Nawaf A.T. and Abdulmajeed B.A. (2024). Design of oscillatory helical baffled reactor and dual functional mesoporous catalyst for oxidative desulfurization of real diesel fuel, *Chemical Engineering Research and Design*, **209**, 193–209, doi: 10.1016/j.cherd.2024.07.032.
- Pinoargote-Chang M.H. *et al.* (2022). Photo-Fenton process for the degradation of blue 1 dye and estradiol benzoate hormone in binary system: Application of sunlight and UV-C radiation, *Case Stud. Chemical and Environmental Engineering*, **6**, 0–5, doi: 10.1016/j.cscee.2022.100226.
- Rashid A.H., hassan A.A, Hadi R.T. and Naje R.T. (2020). Treatment of oil content in oilfield produced water using chemically modified waste sawdust as biosorbent, *Ecology, Environment and Conservation*, **26**(4), 1563–1571.
- Sultan H.K., Aziz H.Y., Maula B.H., Hasan A.A. and Hatem W.A. (2020). Evaluation of Contaminated Water Treatment on the Durability of Steel Piles, *Advances in Civil Engineering*, **2020**, 1269563.
- Xu S. and Lee T. R. (2021). Fe<sub>3</sub>O<sub>4</sub> Nanoparticles : Structures , Synthesis , Magnetic Properties, Surface Functionalization, and emerging applications. *Applied Sciences*, **11**(23), 11301.